Q. J. R. Meteorol. Soc. (1998), **124**, pp. 2299–2327

An extreme cold surge over the Greek peninsula

By K. LAGOUVARDOS*, V. KOTRONI and G. KALLOS
University of Athens, Greece

(Received 31 July 1997; revised 19 February 1998)

SUMMARY

This paper is devoted to the detailed description of an extreme cold surge that occurred 3–13 March 1987, over Greece. This event has been rated as the worst snowfall over the last 100 years and, due to its severity and persistence, it paralysed the economic and communal life of Greece for several days. Emphasis is given to the initiation phase of this event. The structural evolution of the cold surge is analysed using both observations and model results. Model simulations, performed with the Colorado State University–Regional Atmospheric Modelling System, provided the necessary data to diagnose the mesoscale structure of the cold outbreak.

Different mechanisms involved in the structural evolution of the cold surge are investigated. The gustiness of the observed winds and their significant departure from geostrophy are related to the role of an important isallobaric wind. The progression of this surge presented characteristics of a density current, while near the eastern slopes of the mountain barriers of continental Greece cold-air damming occurred, leading to an accelerated flow parallel to the mountains.

KEYWORDS: Balkan fronts Cold-air damming Cold surge Density current

1. INTRODUCTION

Heavy snowfall events over Greece are often associated with cold-air surges propagating from northern and central Europe through the Balkans (Metaxas 1978; Livada-Tselepidaki 1979; Prezerakos and Angouridakis 1984). These cold surges are accompanied with the passage of a fast moving cold front from the north towards the south, very strong winds, especially in the gaps between mountains in northern Greece and over the Aegean Sea, a sharp temperature decrease over the whole country and a sharp pressure rise. The lifetime of these surges is normally from 1 to 3 days, extending up to 10 days in exceptional cases. Their persistence can cause important problems in economic life, since the resulting snowfall can prohibit road transportation on the main traffic routes. Greek forecasters call these cold fronts 'Balkan fronts' due to their origin. In the frame of this study this terminology will be retained, although the classical term 'cold surge' will also be used interchangeably. The forecast of the evolution of these fronts as well as the persistence of cold surges over Greece is of great importance, not only for the impact of snowfall on economic life but also for the safety of navigation in the Aegean Sea in gale force winds.

Cold surges accompanied by severe weather phenomena have also been reported in the Himalayan region (Nakamura and Murakami 1983), over the USA (e.g. Bell and Bosart 1988; Colle and Mass 1995) as well as over Central America (Schultz *et al.* 1997). All the aforementioned studies underlined the fact that cold surges are accompanied by strong lower tropospheric northerly winds, sharp decreases in temperature and sharp pressure rises. In these studies some interesting features accompanying cold surges were also addressed, mainly cold-air damming near mountain barriers as a result of the interaction of the synoptic-scale flow with topography. Bell and Bosart (1988) concluded that the component of the pressure gradient force parallel to the mountain was the primary cause for the appearance of an accelerated flow nearly parallel to the mountains. Colle and Mass (1995) demonstrated that pressure ridging east of the mountain barrier caused ageostrophic northerly winds, while cold avection of upslope flow led to the damming of cold air. Schultz *et al.* (1997) showed that the extraordinary equatorial extent of a cold surge was aided by topographic channelling similar to cold-air damming.

* Corresponding author: University of Athens, Laboratory of Meteorology, Bldg. PHYS-V, Panepistimioupolis, 15784 Athens, Greece.

This study is devoted to the analysis of a severe cold surge over Greece, starting on 3 March 1987, accompanied by heavy snowfall (the snow depth exceeding 2 m in some mountain areas), and strong surface winds especially during the initiation phase of the cold surge over northern Greece (3–4 March). The lifetime of the cold surge was approximately 10 days. Greek forecasters describe this event as the worst cold surge to have occurred over Greece in the last 100 years. The extreme snowfall paralysed the economic life of northern Greece and interrupted road communication between northern and southern Greece for several days.

Despite the exceptional intensity of the surge and the impact that such a phenomenon had on economic and community life, there has so far been no detailed examination of its structural evolution and dynamics. To address this deficiency, this paper provides a detailed investigation of this cold surge. The objectives of this research are the following:

- to document the propagation of this extraordinary cold surge over Greece, based on available observations;
- to further investigate the detailed structure of the cold surge and the progression of the Balkan front based on atmospheric model simulations.

Although the intensity of the phenomena (persistence of low temperatures and snowfall) was remarkable throughout the 10-day period, this study is deliberately limited to the investigation of the initiation phase which presented the most severe weather at the surface. The synoptic description of the cold surge is based mainly on gridded analyses at pressure levels, provided by the European Centre for Medium-Range Weather Forecasts (ECMWF), with $1^\circ \times 1^\circ$ latitude–longitude resolution. The mesoscale analysis of the surge as well as the description of the Balkan front structure are based on nested-grid simulations performed with the Colorado State University–Regional Atmospheric Modelling System (RAMS).

This paper is organised as follows. In section 2, a synoptic overview of the cold-surge event is given, based on observations and on ECMWF gridded analysis data. Special emphasis is given to the initiation stage of the surge (3–4 March 1987). The role of the isallobaric component of the ageostrophic wind in the modification of lower tropospheric winds is also discussed. Section 3 provides a short description of the RAMS model used in this study as well as of the specific set-up used for the performed simulation. Section 4 is devoted to the discussion of the model results. The behaviour of the surge, reminiscent of a density current, as well as the damming of cold air to the east of the mountain barriers on the eastern coasts of continental Greece is also investigated. The concluding discussion is given in section 5.

2. Overview of the cold surge (3–4 March 1987)

The cold surge analysed in this study affected the Greek peninsula during the period 3 to 13 March 1997. The analysis is mostly focused on weather conditions during the initiation stage of the cold surge (from 0000 UTC 3 March 1987 through 1200 UTC 4 March 1987). However, a brief description of the mature stage of the phenomenon is also given. This overview will be based on the ECMWF gridded uninitialised analyses on pressure levels, with a horizontal resolution of $1^\circ \times 1^\circ$. The position of the fronts over the area of interest has been analysed subjectively, based on the location of strong wind and temperature gradients. However, this procedure was assisted by the objective frontal analysis technique proposed by Hewson (1996). This analysis is based on the mathematical and graphical process of the equivalent-potential-temperature field at the 850 hPa level.

(*a*) *Synoptic analysis of the cold surge initiation stage*

The surface analysis at 0000 UTC 3 March 1987 (Fig. 1(a)) shows a low centre of 998 hPa over northern Italy, while over the eastern Atlantic a high-pressure system of 1030 hPa prevails. The frontal discontinuity over the Balkans (termed Balkan front hereafter) has an east–west orientation, following approximately the 43°N latitude line. At the 850 hPa level (Fig. 1(b)), geopotential height and temperature analyses show the existence of low geopotential heights over Russia and the Balkans, while in general the areas located north of 45°N are influenced by negative temperatures. The temperature gradient is concentrated within a curved belt extending from the area north-east of the Alps to the Black Sea. The 500 hPa chart shows a cut-off low centred at 53°N, 30°E, while a ridge has developed over the eastern Atlantic and the British Isles, with its axis oriented approximately north–south (Fig. 1(c)). A very strong jet streak with a maximum speed of 74 m s^{-1} is observed at the 250 hPa level, associated with the confluent flow over central France. The southern flank of the cut-off low over Russia is also associated with a strong jet streak, with a maximum speed of 52 m s^{-1} at 400 hPa, located north of the Black Sea.

Twelve hours later (1200 UTC 3 March) the low centre, which was located over northern Italy at 0000 UTC, has progressed over the maritime area between Italy and Greece. This low centre is associated with a cold front which at that time is over the Greek peninsula, producing moderate precipitation mainly over south-western Greece and the Aegean Sea. At the same time, the Balkan front becomes more organised with a west–east orientation almost along latitude 41°N (Fig. 2(a)). At the 850 hPa level (Fig. 2(b)) there is a significant packing of the isotherms over the Balkans and the Black Sea, associated with important cold-air advection. Cold-air advection from the north is also evident over France and the Benelux. The 0 °C isotherm has drifted southwards, mainly in the area from 10°E to 30°E approximately 300 km to the south of its 0000 UTC position; it is found over the northern borders of Greece, while it remained quasi-stationary in the area west of 10°E. Up to that time and until 2100 UTC the surface synoptic network over northern continental Greece and the northern Aegean Sea reported a progressive decrease in surface pressure of the order of 6 hPa, a 2 degC decrease in surface temperature and a gradual wind speed increase (with winds exceeding 20 m s^{-1} at some stations at 2100 UTC). Surface synoptic reports will be discussed in more detail later in this section.

At 500 hPa, the ridge line over the British Isles has progressed slightly eastwards, while high geopotential heights are evident over the British Isles (Fig. 2(c)). The cut-off low centre over Russia has also moved eastwards without deepening, while a minor trough line has developed over the sea south of Italy. This trough line is associated with the surface low centre depicted in Fig. 2(a). The jet streak associated with the ridge has moved south-east over the western Mediterranean with a maximum wind speed of 68 m s^{-1} at 250 hPa over Sardinia. The jet streak axis associated with the cut-off low has shifted northwards with a maximum wind speed of near 60 m s^{-1} at 400 hPa north of the Black Sea.

Perhaps the most dramatic changes in low-level features during the analysed event occurred at 0000 UTC 4 March. At the surface, the low centre and the associated frontal activity has moved over the southern Aegean Sea while the Balkan front has progressed farther south over central Greece (Fig. 3(a)). The Balkan front is also depicted in the packing of 850 hPa isotherms over the area, and it is positioned 350 km southwards from its 1200 UTC 3 March position (Fig. 3(b)). Note that the strongest temperature gradients (14 degC over 180 km) are found over eastern Greece, slightly to the west of the 30°E meridian. At 500 hPa the ridge over the Atlantic and the British Isles has moved slightly eastwards, and the ridge line has turned clockwise having a more south-west to north-east orientation. The cut-off low centre over Russia has progressed slowly north-eastwards,

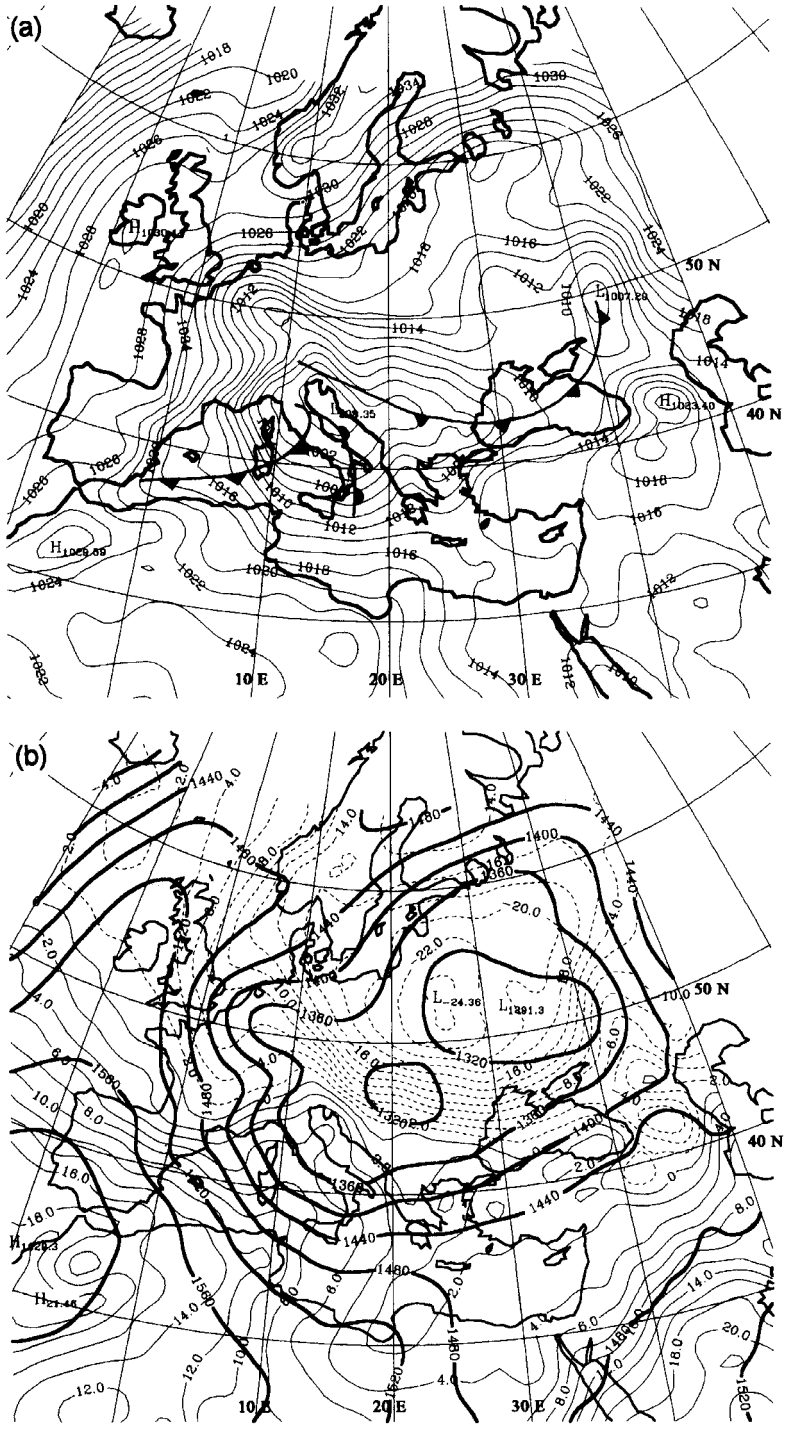

Figure 1. ECMWF analyses valid at 0000 UTC 3 March 1987. (a) Mean sea-level pressure (2 hPa intervals); (b) 850 hPa geopotential height (bold line, 40 m intervals) and temperature (solid line, 2 degC intervals, negative values are dashed); (c) 500 hPa geopotential height (40 m intervals) and isotachs at level of maximum wind (light shading: >50 m s^{-1}, medium shading: >60 m s^{-1}, dark shading: >70 m s^{-1}). Level of maximum wind is at 400 hPa over Russia and 250 hPa over Western Europe and the Mediterranean Sea.

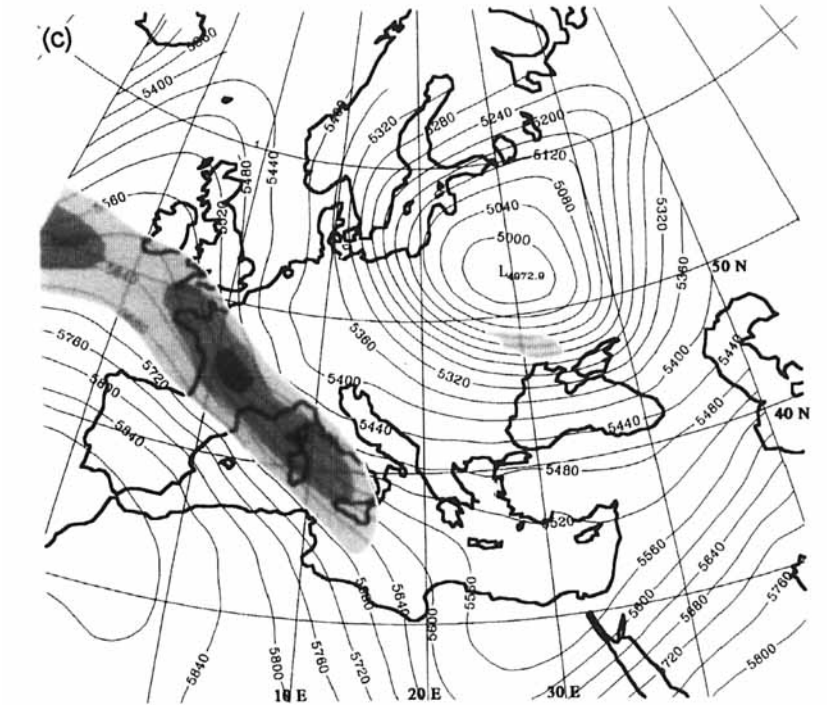

Figure 1. Continued.

while the trough line over Greece is now oriented along the 22°E meridian. The jet streak at the 250 hPa level over the western Mediterranean has been divided into two distinct parts: the first with a north–south orientation located over France and the western Mediterranean with a maximum wind speed of 58 m s^{-1}; and the second with a north-west to south-east orientation over the central Mediterranean and a maximum wind speed of 62 m s^{-1} over the Gulf of Sidra (Fig. 3(c)). Inspection of the upper-level divergence (not shown) did not reveal any significant ageostrophic flow around the exit region of the jet streak.

At 1200 UTC 4 March, the high-pressure system over Western Europe has progressed south-eastwards, and the Balkan front has progressed rapidly further southwards and affected the whole Greek peninsula (Fig. 4(a)). Indeed, severe weather with snowfalls and strong northerly winds was produced over northern and central Greece and the Aegean Sea. At 850 hPa the 0 °C isotherm has drifted southwards and is found north of Crete, along latitude 36°N in the area from 10°E to 30°E, while it still remains stationary west of 10°E and east of 25°E (Fig. 4(b)). An organised trough oriented north–south affects the area from the Balkans through the Greek peninsula at the 500 hPa level, while a 65 m s^{-1} jet streak is evident over the north African coast at the 250 hPa level (Fig. 4(c)).

The progression of the Balkan front over northern Greece is reflected in the reports from the surface synoptic network in the area. Figure 5 presents a time series of 3-hourly reports from Limnos island in the northern Aegean Sea (the coordinates of the station are 39°55′N, 25°14′E). Indeed, a temperature drop of 9 degC and a surface pressure increase of 5.3 hPa were reported between 2100 UTC 3 March and 0000 UTC 4 March; the 6 h pressure rise ending at 0300 UTC 4 March exceeded 10 hPa, while the 12 h pressure rise ending at 0900 UTC 4 March exceeded 16 hPa. This latter considerably exceeds the 10 hPa pressure rise within 12 h reported by Colle and Mass (1995) as a criterion for the determination of

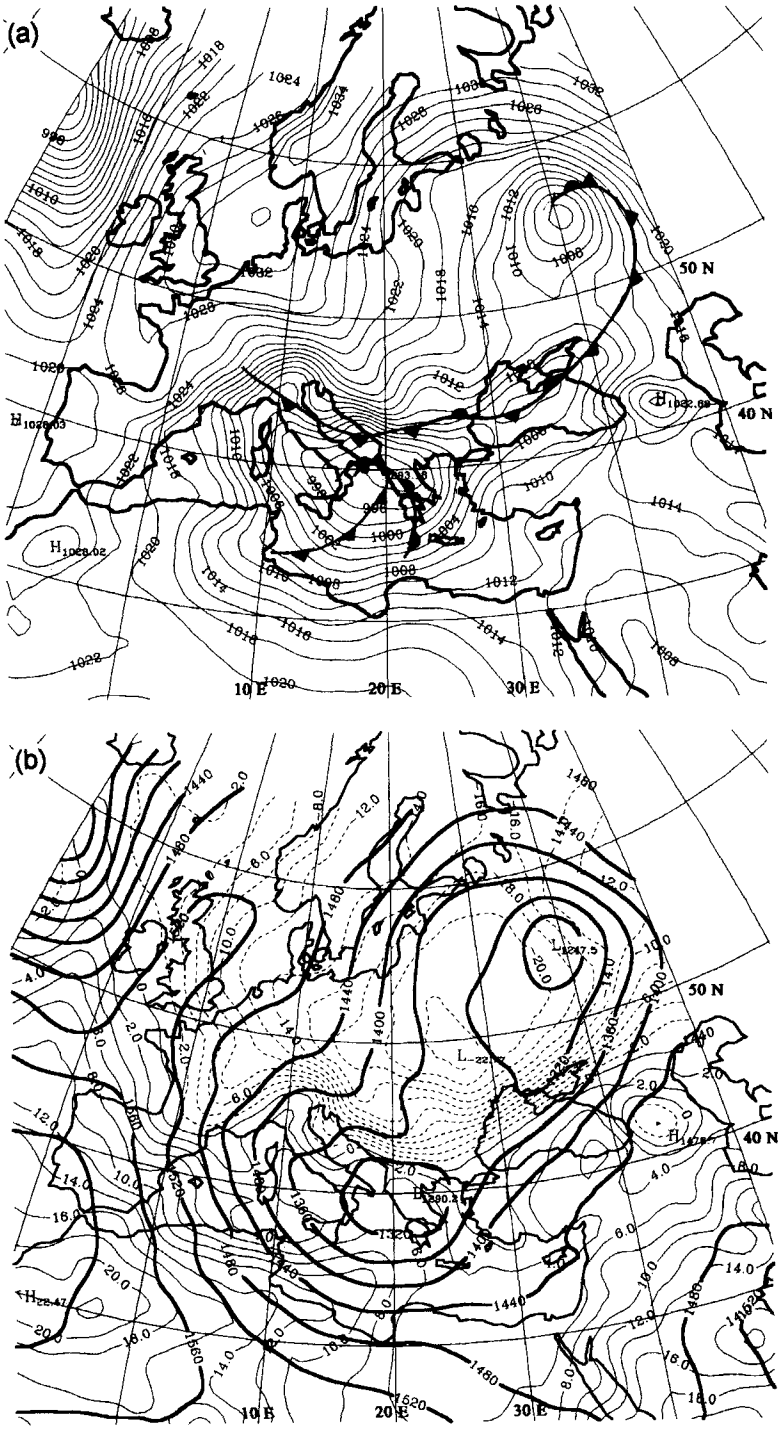

Figure 2. As Fig. 1 except at 1200 UTC 3 March 1987.

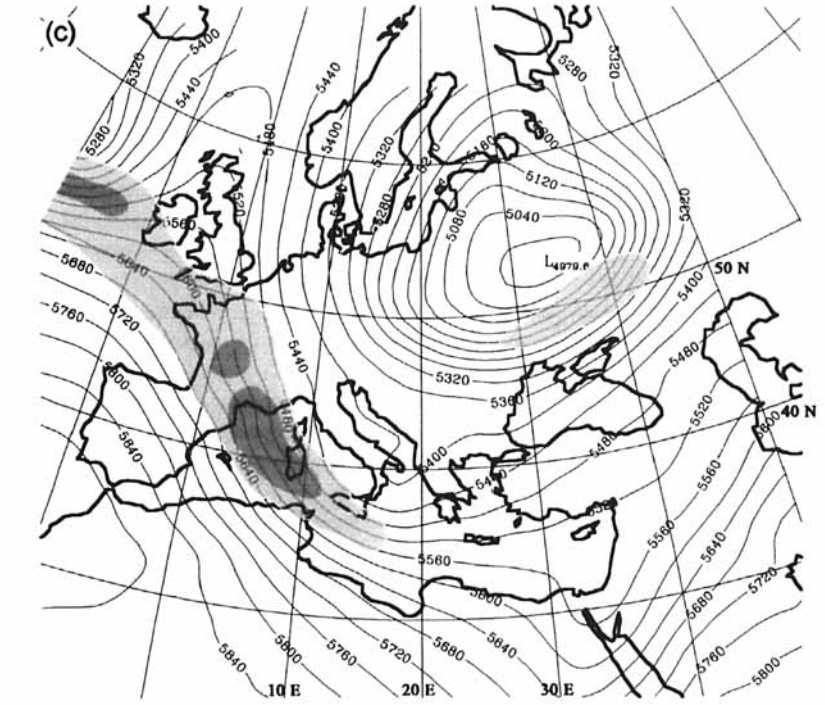

Figure 2. Continued.

cold surges over the US Great Plains. Moreover, surface winds increased from 12–14 m s^{-1} ahead of the Balkan front to 23 m s^{-1} behind it (at 0000 UTC 4 March and almost up to 0900 UTC) with gusts of 33 m s^{-1}. During the early morning hours of 4 March snowstorms were reported over northern Greece and affected central Greece later on the same day.

Prezerakos and Angouridakis (1984) performed a climatological analysis of the synoptic patterns resulting in extreme snowfall in Athens, based on the study of mean sea-level pressure, 500 hPa height, and 500–1000 hPa mean thickness charts, and concluded that in general these cases follow two distinct synoptic patterns. The authors stated that for the first synoptic pattern: "The clue system is a long-wave warm high on the 500 hPa charts over north-west Europe, accompanied by a maximum of positive height anomalies. This maximum is a quasi-stationary one and it dominates the flow, governing the way advected polar and/or arctic air masses coming from the Scandinavian countries or from further north reach the Balkans and Greece". The analysed snowstorm of 3–4 March 1987 can be classified as this type of climatological synoptic pattern, although its persistence makes it an outlier of the common climatological patterns.

(*b*) *Brief discussion of the mature stage of the cold surge*

The cold air masses which had been advected over the Balkans and the Greek peninsula were cut off on 6 March. Inspection of a series of maps revealed that the cut-off low evident at 500 hPa, and the cold pool on the 1000–500 hPa thickness maps, remained over the southern Balkans and Greece until 13 March 1987 (not shown). From 8 March there was an intensification of the anticyclonic circulation over Central and Eastern Europe and Russia. Under this situation, cyclogenesis is favoured over the Cyprus area (Metaxas

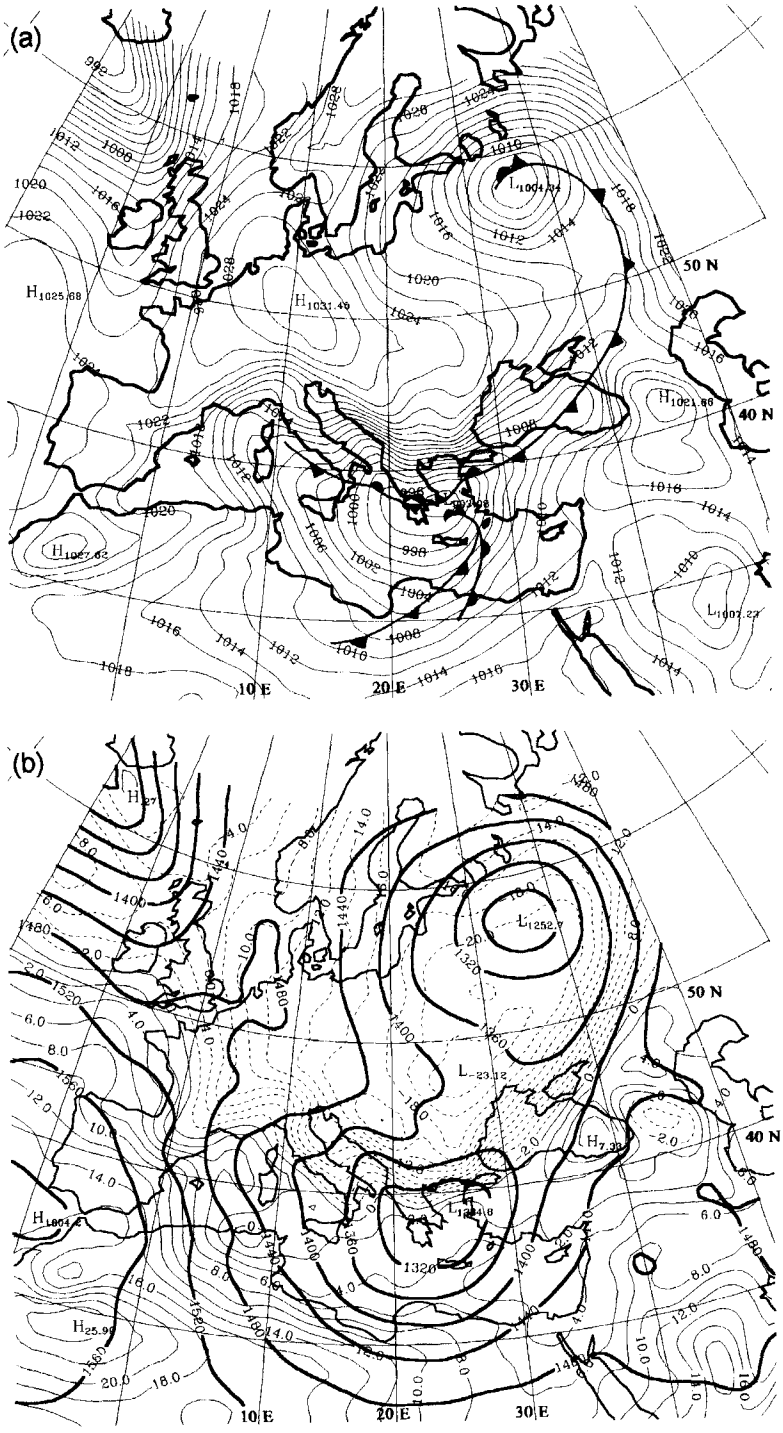

Figure 3. As Fig. 1 except at 0000 UTC 4 March 1987.

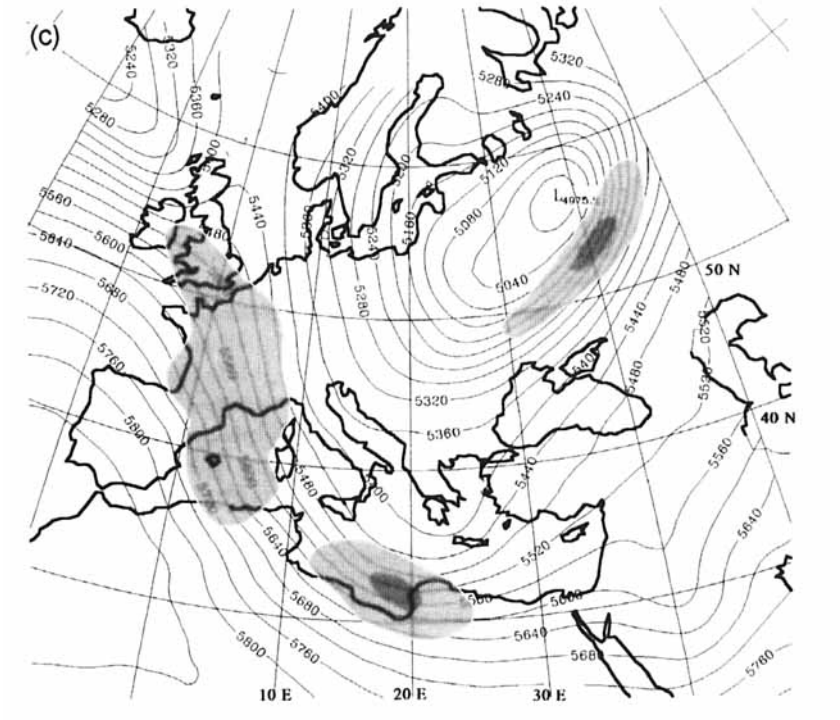

Figure 3. Continued.

1978; Kallos and Metaxas 1980). At 0000 UTC 9 March the cut-off low reached the lowest temperatures of the 10-day period, less than −40 °C at the 500 hPa level over Greece (not shown). This cut-off low over the Greek peninsula resulted in consecutive days with snowfall over almost all of continental Greece. From 4 to 13 March, 7 days of snow were reported in Athens (37°58′N, 23°46′E) and 5 days in Thessaloniki (40°38′N, 22°58′E), while non-coastal stations reported snow almost every day during the same period. From 12 March, the anticyclonic circulation over Europe weakened and the cut-off low drifted eastwards, gradually dissipating.

(c) *Reports from the surface synoptic network during the initiation stage*

The progression of the cold surge towards the south can also be depicted through a series of surface synoptic reports over the Balkans. At 1200 UTC 3 March 1987, the Balkan front was located approximately over the northern Greek borders, with the lowest temperatures (below 0 °C) reported over southern Serbia and northern Bulgaria (Fig. 6(a)). The wind field over the Ionian Sea was from a south-western direction, associated with a belt conveying warm and moist air masses (the 'warm conveyor belt', as termed by Browning and Pardoe 1973) ahead of the cold front located offshore of western Greece. At that time moderate precipitation was reported mainly by stations over south-western Greece and the Aegean Sea. Snow was reported by the surface stations experiencing negative temperatures. At 1800 UTC 3 March, warm and moist air masses covered the major part of the Aegean Sea (Fig. 6(b); note that for clarity dew-point temperatures are only plotted over the sea), while the Balkan front is over northern Greece. By 0000 UTC 4 March, the cold outbreak almost reached the northern part of the country. Almost all

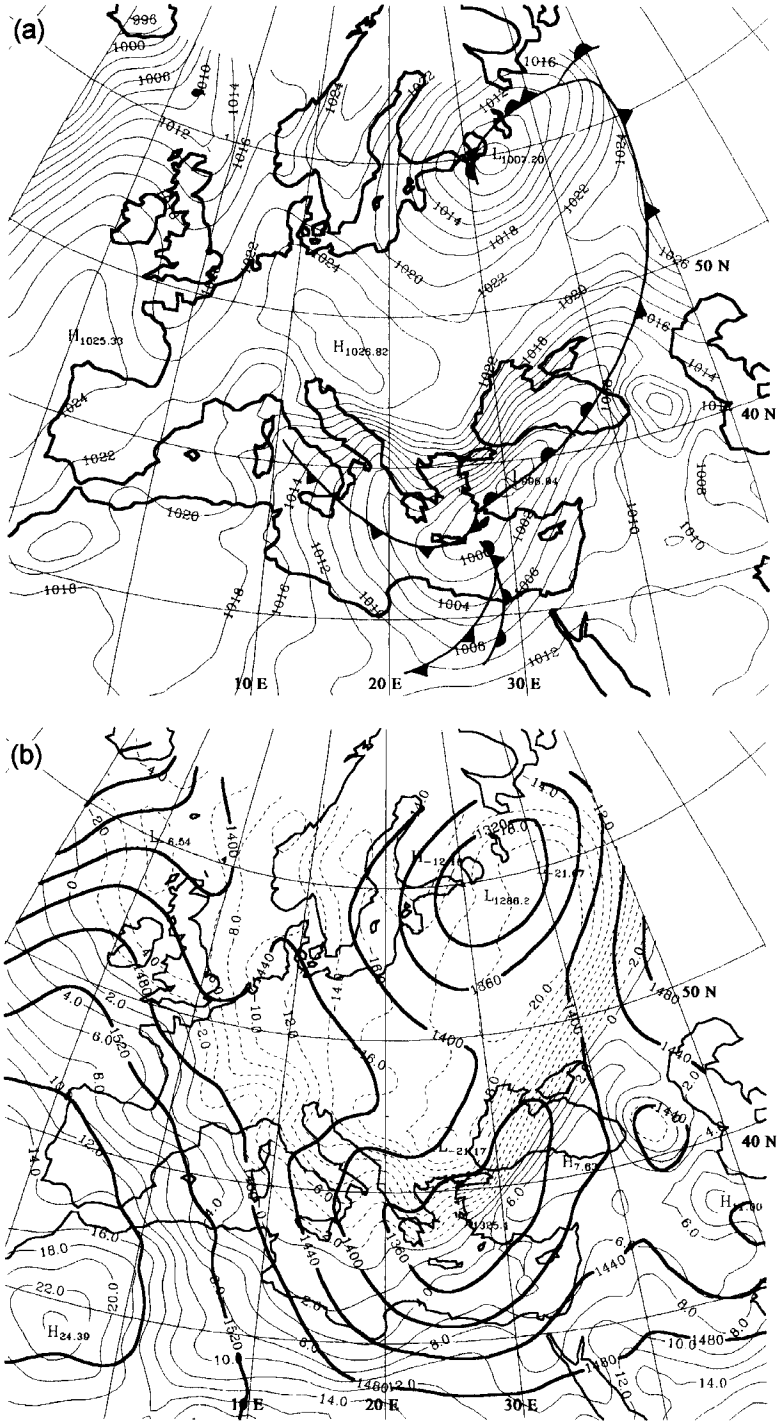

Figure 4. As Fig. 1 except at 1200 UTC 4 March 1987.

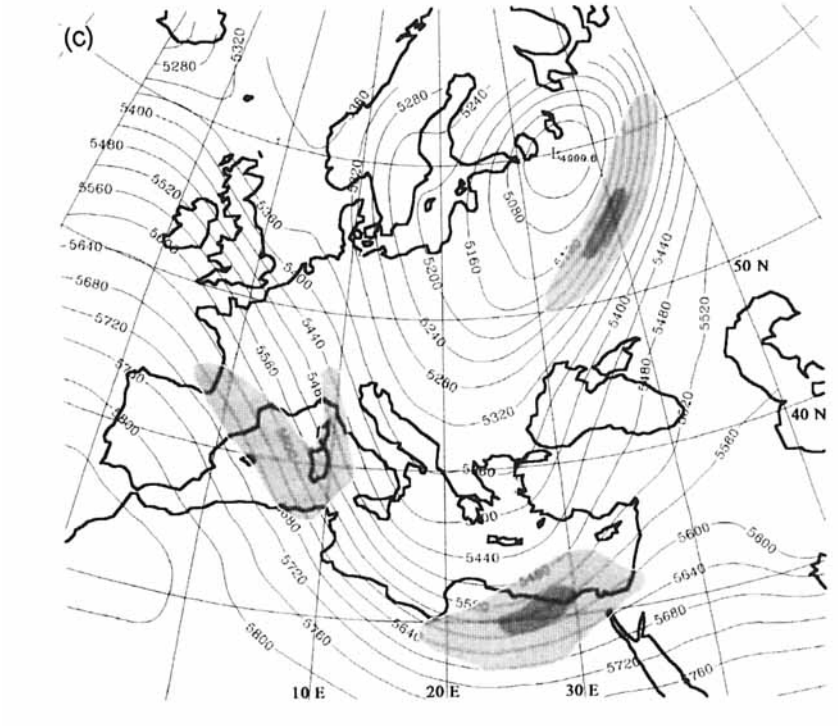

Figure 4. Continued.

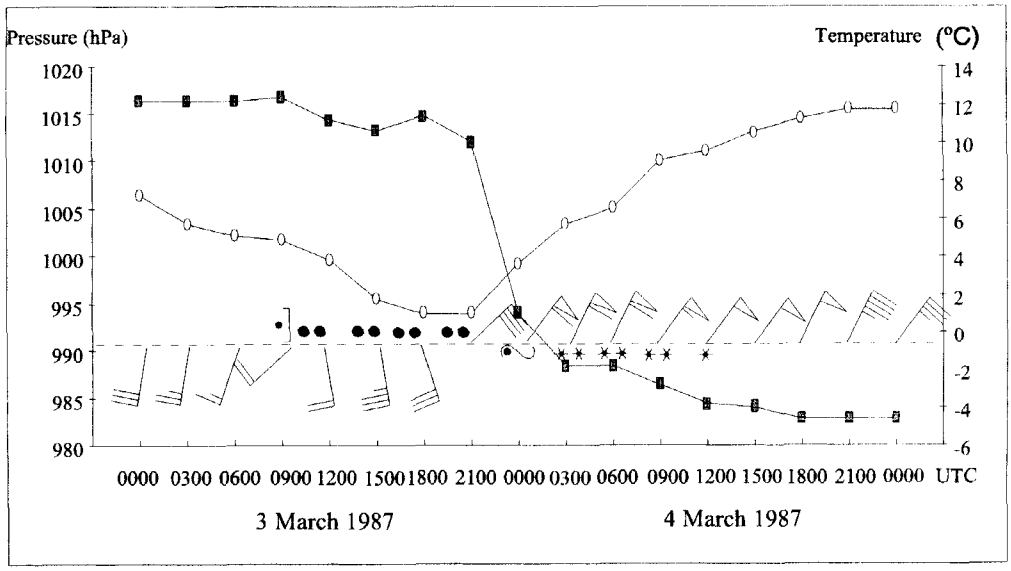

Figure 5. Temporal variation of mean sea-level pressure (open circles); temperature (solid rectangles); wind (one pennant equals 20 m s^{-1}, one barb 4 m s^{-1} and one half-barb 2 m s^{-1}) and current weather (conventional symbols) at Limnos Island in Northern Aegean Sea.

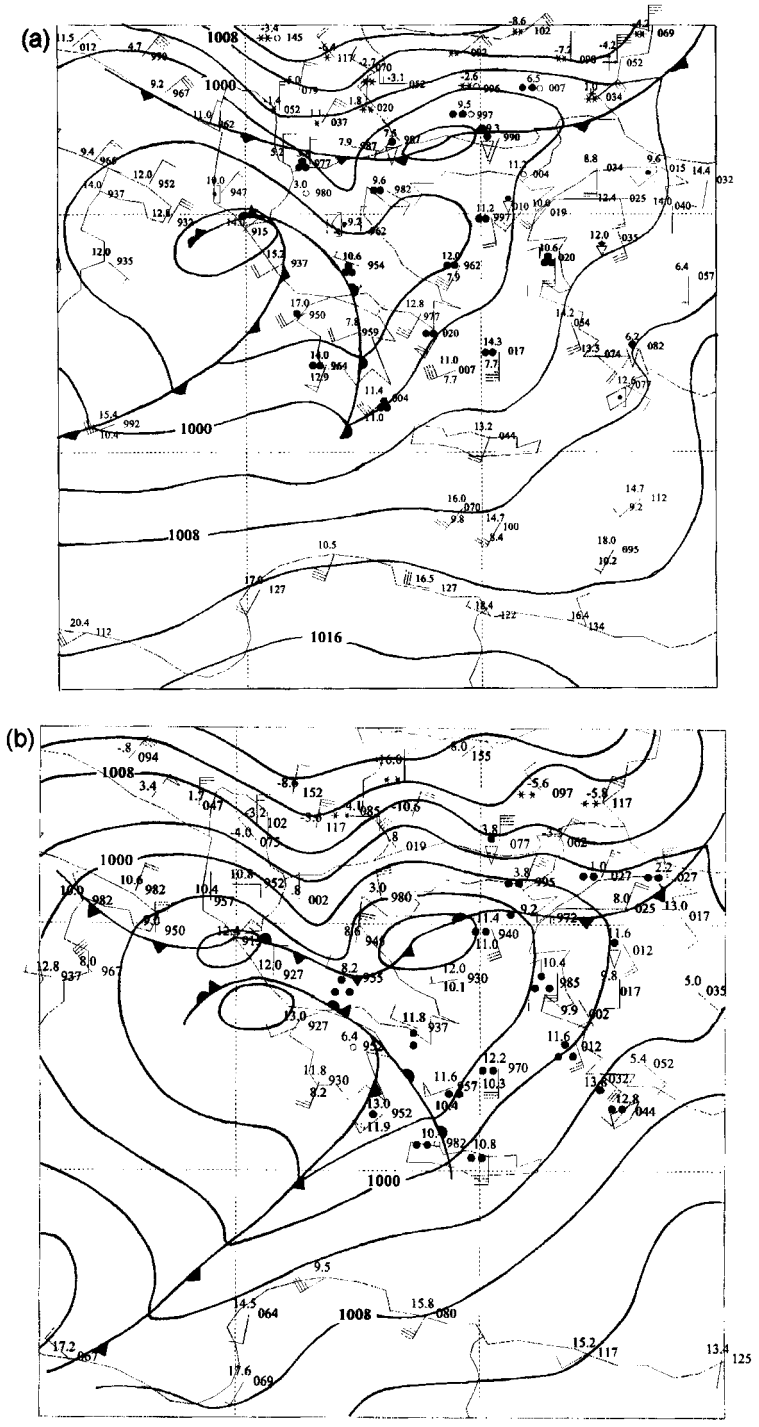

Figure 6. Surface synoptic reports of mean sea-level pressure (in tens of hPa, with the leading 10 or 9 omitted), temperature, dew-point temperature (only for selected stations over the sea), current weather (conventional symbols) and wind (one pennant equals 20 m s^{-1}, one barb 4 m s^{-1} and one half-barb 2 m s^{-1}). Isobars are plotted at 4 hPa intervals. (a) 1200 UTC 3 March 1987; (b) 1800 UTC 3 March 1987; (c) 0000 UTC 4 March 1987, LI shows the location of Limnos Island, and AL Alexandroupolis; (d) 0600 UTC 4 March 1987; (e) 1200 UTC 4 March 1987.

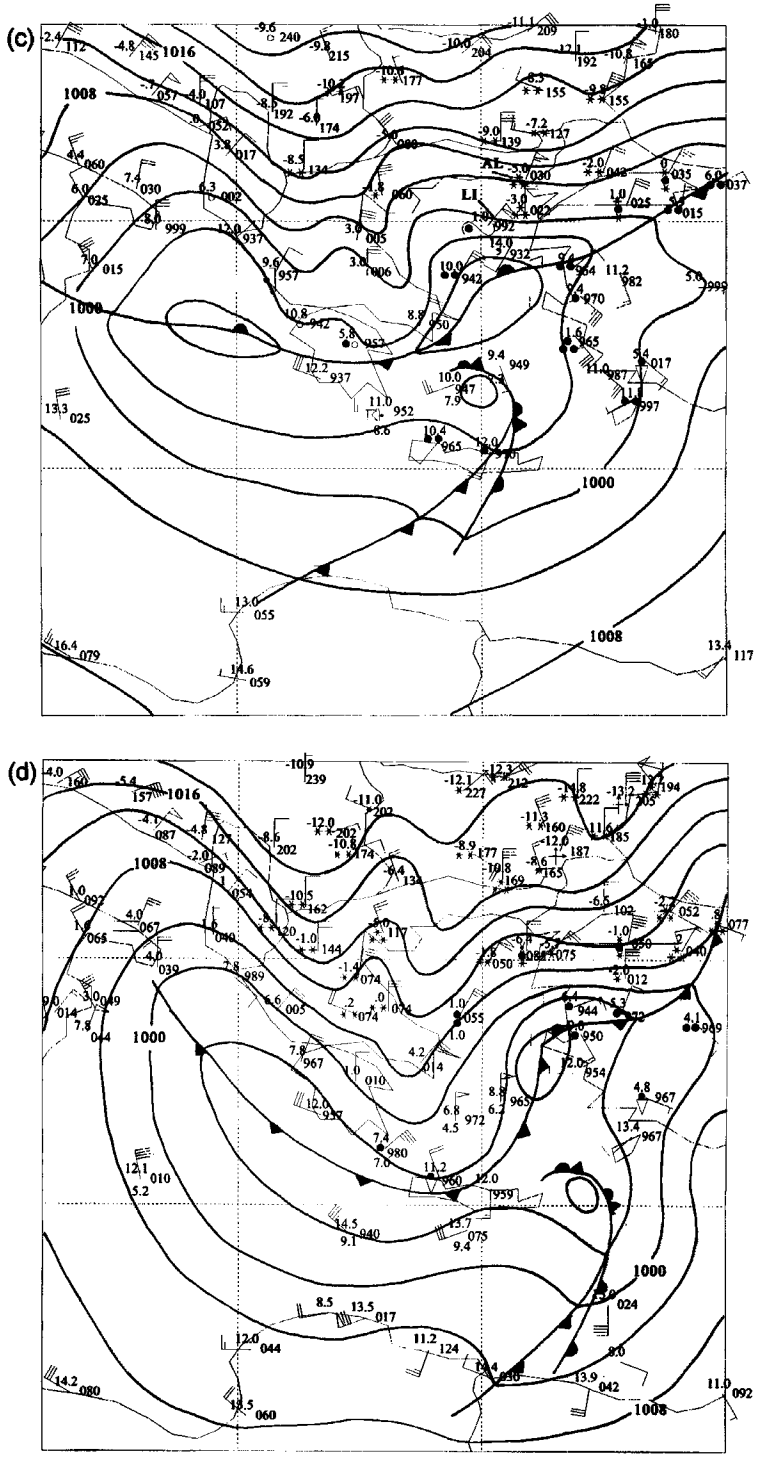

Figure 6. Continued.

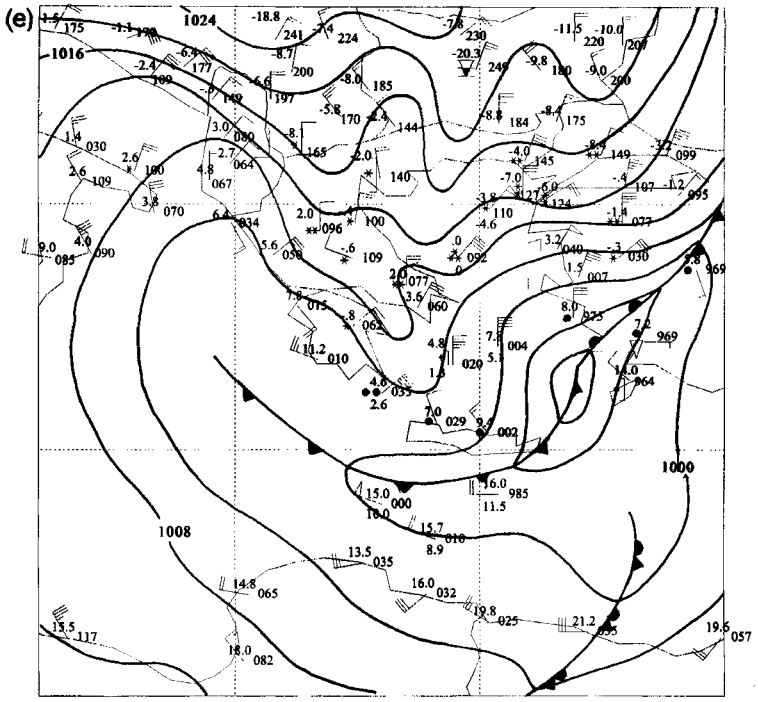

Figure 6. Continued.

stations north of 40°N report negative temperatures and snowfall, except over Albania, and southern Italy (Fig. 6(c)). Figure 6(c) depicts two main characteristics of the pressure and temperature fields.

• An abrupt change in temperature and wind over the northern Aegean Sea, following a narrow zone oriented south-west to north-east. The strongest surface north-easterly winds are reported from Limnos Island (24 m s^{-1}; LI in Fig. 6(c)) and Alexandroupolis (22 m s^{-1}; AL in Fig. 6(c)). These strong winds are highly ageostrophic (the relationship of the sharp wind increase to the rapid pressure changes and the wind departure from geostrophy, are discussed in the following sub-section). Just south-east from Limnos a ship reported 14 °C with a 4 m s^{-1} south-westerly wind, indicating the existence of a very sharp temperature gradient associated with the Balkan front over the northern Aegean Sea.

• A ridge of high pressure over the eastern coasts of continental Greece, roughly parallel to the Olympus and Ossa mountain barrier, while a second less pronounced high-pressure ridge is evident east of Pindos (for the topography of the region see Fig. 8(b)). Both the above structures (sharp temperature gradients and pressure ridging) will be discussed in section 4, using results from RAMS nested-grid simulations.

By 0600 UTC 4 March 1987 the Balkan front reached southern Greece; winds with northerly components were observed over the Aegean Sea, while temperatures near 0 °C and snow are also reported by stations south of 40°N (Fig. 6(d)). Six hours later (1200 UTC 4 March, Fig. 6(e)) the Balkan front had progressed just south of Crete, associated with negative temperatures over eastern continental Greece and the central Aegean, and very strong north to north-easterly winds over the Aegean Sea. Note also that three ships south of Crete, just ahead of the Balkan front, reported temperatures exceeding 15 °C; these

contrast with the low temperatures reported behind it, and indicate that the Balkan front is still characterized by strong cross-front thermal gradients as it propagates southwards. Snow was reported by a surface station located north of Athens, while 3 hours later snow was also reported at Athens airport.

(*d*) *Role of the isallobaric component of the ageostrophic wind*

As mentioned in the last sub-section, the progression of the Balkan front over the Greek peninsula was associated with gusty winds and heavy snowstorms mainly in the northern part of the country. As can be seen in Figs. 5 and 6(c), the synoptic surface network at 0000 UTC 4 March reported winds of 24 m s^{-1} over Limnos island and 22 m s^{-1} over north-eastern Greece from a north-easterly direction, while over northern and central Greece the reported winds are of the order of 14 m s^{-1} from the north. Inspection of the mean sea-level pressure field and of the reported surface winds (Fig. 6(c)) shows that over the northern Aegean Sea and the Dardanelles straits the observed winds are strongly ageostrophic.

The severity of the snowstorm onset was strongly related to the rapid progression of the Balkan front southwards and the associated rapid change of surface pressure. Indeed, in the climatological study of Prezerakos and Angouridakis (1984) it was pointed out that the onset of these gusty winds is related to an important isallobaric component of the ageostrophic wind.

The isallobaric component v_i of the ageostrophic wind, assuming negligible horizontal variations of density, is defined as (Bluestein 1993):

$$v_i = -\frac{1}{\rho f^2}\nabla_z\left(\frac{\partial p}{\partial t}\right) \tag{1}$$

where ρ is the density of the air, f is the Coriolis parameter, and p and z denote pressure and height, respectively.

In order to derive a gridded field of the isallobaric wind, 6-hour mean sea-level pressure tendencies ending at 0000 UTC 4 March 1987, derived from the ECMWF mean sea-level pressure analysis files, have been used. Figure 7 shows the isallobaric wind at 0000 UTC 4 March, superimposed on the mean sea-level pressure field and the 6-hour pressure tendency. A maximum of 8.8 hPa of positive pressure tendency is evident over northern Greece and isallobaric winds are pointing away from this positive pressure tendency centre. The isallobaric wind over the northern Aegean Sea is of the order of 12–14 m s^{-1}, and even 16 m s^{-1} at the exit of the Dardanelles straits. The north to north-east winds, reported by the surface network over the northern part of Greece (Fig. 6(c)) are oriented almost perpendicular to the isobars, and thus are highly ageostrophic. This departure from an easterly geostrophic flow can be attributed to the strong north-western isallobaric wind over the northern Aegean Sea. Forbes *et al.* (1987) also identified the isallobaric wind (together with surface friction) as the main source of departure from geostrophy to explain the large cross-isobaric angle of the surface wind east of the Appalachian Mountains (USA). The orientation of the winds almost normal to the isobars creates strong convergence towards the low centre, thus enhancing ascent. The existence of moist air masses (see Fig. 6(b)) ahead of the approaching cold surge provided the necessary moisture source for precipitation, which at that time fell almost entirely as snow at ground level.

3. Model description and set-up

RAMS has been developed at Colorado State University and the ASTER Division of Mission Research Corporation. It was developed as a research model, but has also recently

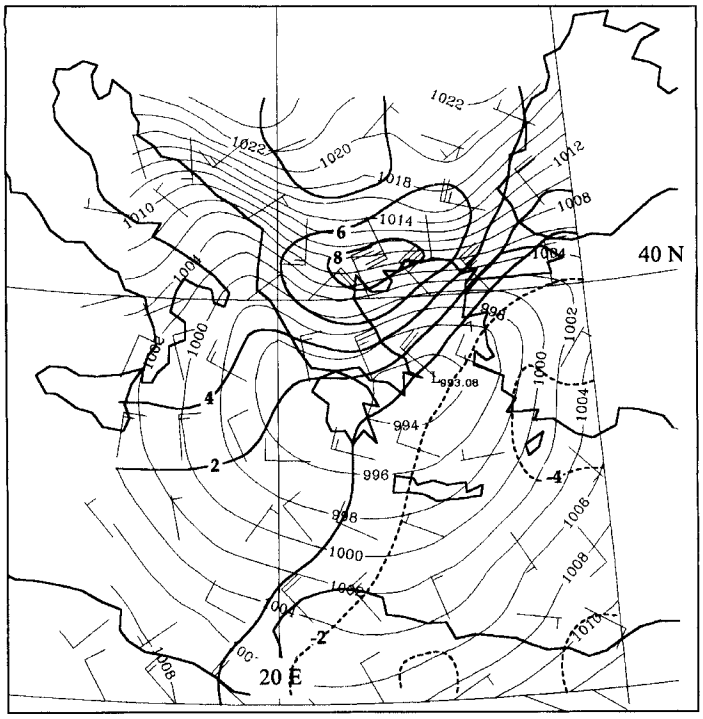

Figure 7. ECMWF analysis of mean sea-level pressure (plotted every 2 hPa), valid at 0000 UTC 4 March 1987 and the isallobaric component of the ageostrophic wind calculated from 6-hour pressure tendencies ending at 0000 UTC 4 March; one barb equals 4 m s^{-1} and one half-barb 2 m s^{-1}. Six hour pressure tendency is superimposed at 2 hPa 6 h^{-1} intervals (positive values are in bold solid lines and negative in dashed bold lines).

started to be used operationally (e.g. Cotton *et al.* 1994; Tremback *et al.* 1994). A general description of the model and its capabilities is given in Pielke *et al.* (1992). However, some RAMS features are summarized in the following:

- two-way interactive nested grid structure (Clark and Farley 1984);
- terrain-following coordinate surfaces with cartesian or polar stereographic horizontal coordinates;
- cloud microphysics parametrization at various levels of complexity (Walko *et al.* 1995).
- modified Kuo cumulus parametrization (Tremback 1990);
- radiative-transfer parametrizations (short- and long-wave) through clear and cloudy atmospheres (Chen and Cotton 1987);
- various options for upper and lateral boundary conditions and for finite operators;
- various levels of complexity for surface-layer parametrization (soil-layer moisture and temperature model, vegetation parametrization etc., McCumber and Pielke 1981; Avissar and Mahrer 1988).

For the present application, RAMS was initialised at 0000 UTC 3 March 1987 and the duration of the simulation was 48 hours. The non-hydrostatic version of the model was employed, using two nested grids: (i) the outer, with a mesh of 76 × 62 points and a 40 km horizontal grid interval, centred at 40°N, 20°E, and (ii) the inner, with 122 × 110 points and a 10 km horizontal grid interval, centred at 39°24′N, 22°24′E. The two nested grids are shown in Fig. 8(a) and the topography of the inner grid in Fig. 8(b).

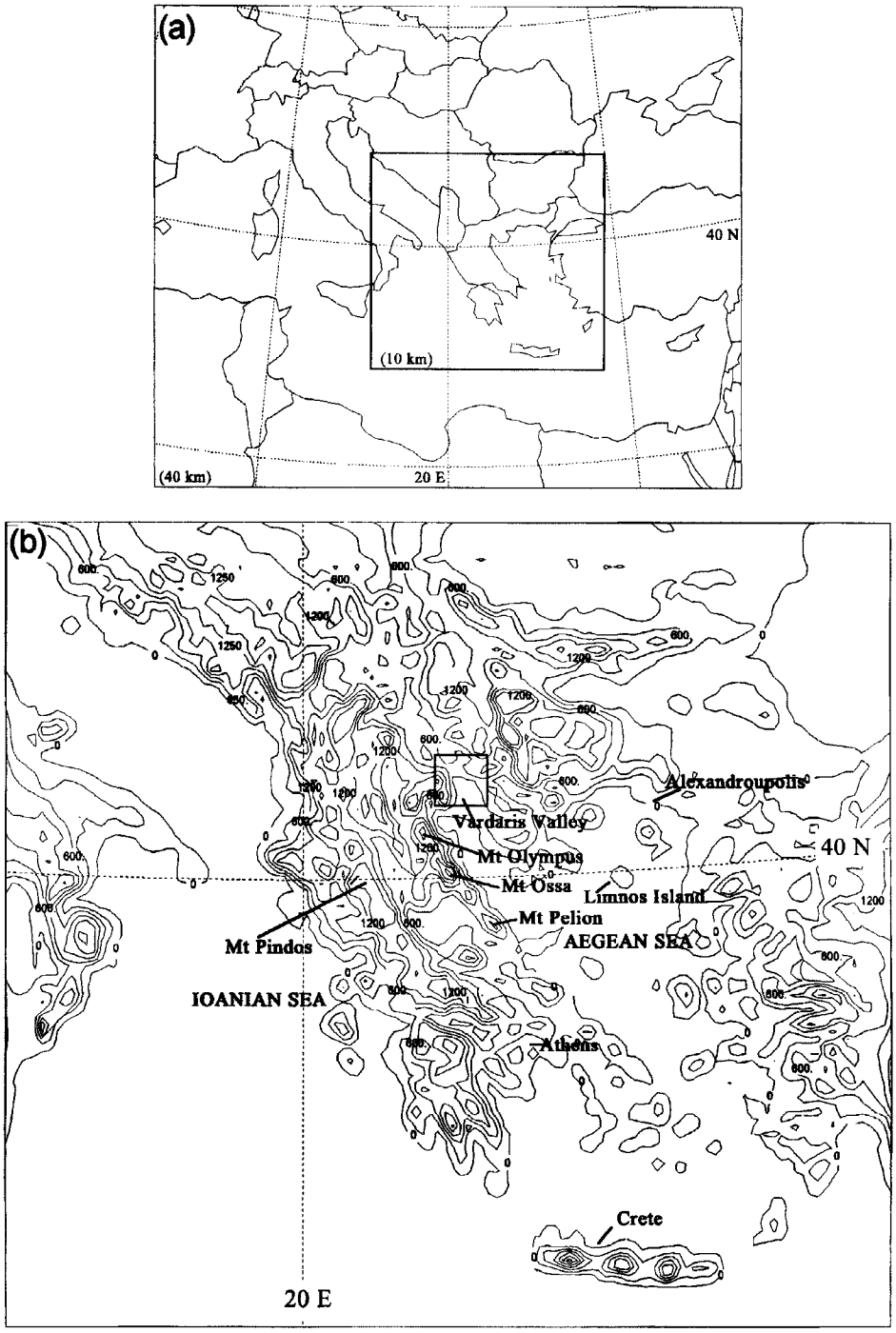

Figure 8. (a) Domain of the two nested grids of RAMS (see text). For each grid, the horizontal grid increment is also given. (b) Topography inside the inner grid of RAMS (contoured at 300 m intervals).

Twenty five levels following the topography were used on both grids. The vertical spacing varied from 120 m near the surface to 1 km at the top of the model domain ($z = 15.5$ km). Together with these settings, other RAMS configuration options include:

- A rigid lid was set at the top model boundary, while 'top-boundary nudging' (which filters out gravity waves) was activated.
- The lateral boundary conditions on the outer grid comprised a relaxation scheme similar to that of Davies (1976).
- A soil layer has been used to predict the sensible- and latent-heat fluxes at the soil–atmosphere interface. Six soil levels have been used down to 50 cm below the surface.
- The full microphysics package of RAMS was activated. This includes the condensation of water vapour to cloud water when supersaturation occurs, as well as the prognosis of rain, graupel, pristine ice, aggregates and snow species.
- A modified Kuo-type cumulus parametrization developed by Tremback (1990) was used because the model-resolved convergence produced on the scales of the outer (40 km) grid is not enough to explicitly initiate convection.

The ECMWF $1^\circ \times 1^\circ$ gridded analysis fields were used in order to initialise the model. The ECMWF data are objectively analysed by the RAMS model on isentropic surfaces, from which they are interpolated to the RAMS grids. The 6-hourly ECMWF analyses were linearly interpolated in time in order to nudge the lateral boundary region of the coarser RAMS grid every hour. Climatological sea-surface temperature data of $1^\circ \times 1^\circ$ resolution and topography derived from a $30'' \times 30''$ terrain data were used. Finally, gridded vegetation-type data of $10' \times 10'$ resolution were used.

4. Model results

(a) *Horizontal structure*

Figure 9(a) shows the RAMS temperature and wind fields at $z = 57$ m above ground level inside the inner grid, at 1200 UTC 3 March 1987 (after 12 hours of model simulation). Strong south-westerly flow is evident south of continental Greece, backing to a southerly direction over the Aegean Sea. The strongest winds (24 m s^{-1}) are reported over the maritime area west and north-west from Crete, just ahead of the cold frontal discontinuity shown in Fig. 2(a). The model-predicted wind field is in very good agreement with the surface observations (Fig. 6(a)), especially in the areas of maximum wind. The RAMS temperature field shows temperature values exceeding 12 °C in a great part of the domain, except over mountainous regions of Greece and the south Balkans, as well as negative values over southern Serbia. This region of negative temperatures, which is also characterized by strong northerly winds, delimits the southern edge of the cold outbreak as this is progressing southwards. It should be mentioned that the RAMS temperature field is also in good agreement with the surface observations (Fig. 6(a)), except over northern Bulgaria where RAMS predicted temperature values are higher than the negative values reported by the synoptic network.

At 0000 UTC 4 March, the progression of the Balkan front over northern and central Greece is obvious (Fig. 9(b)). The major part of northern Greece experiences negative temperatures, with a remarkably sharp contrast of temperature (10 degC over 50 km) and wind speed and direction along a south-west to north-east oriented narrow belt over the northern Aegean Sea near the Dardanelles straits. As mentioned before, this sharp contrast was also evident from the synoptic reports. Indeed, Limnos island reported a temperature of 1 °C and a north-easterly wind of 24 m s^{-1}, while a ship 50 km to the south reported a temperature of 14 °C and a south-westerly wind of 4 m s^{-1} (see Fig. 6(c)). RAMS

predicted the strongest winds over the maritime area around Limnos island in the northern Aegean Sea, exceeding 30 m s^{-1}, in good agreement with the 24 m s^{-1} synoptic report and the wind gusts of 33 m s^{-1} reported by the same station within the period 2100 UTC 3 March to 0000 UTC 4 March. Additionally, the RAMS-predicted wind field reveals an intensification of the wind due to the channelling between the mountain gaps, especially over Vardaris valley north-west of Thessaloniki (for the location of the valley see Fig. 8(b)). The resulting wind is named Vardaris (from the valley name, also found as Vardarac—see Meteorological Office 1962); it is well known as a cold north to north-westerly wind which can at times affect areas farther south over eastern Greece.

By 0600 UTC 4 March (Fig. 9(c)) the 0 °C isotherm has drifted farther south mainly over the northern Aegean Sea, while RAMS also predicted an intensification of winds over almost the whole Aegean Sea. Northerly winds prevail over the northern and central Aegean Sea, in good agreement with the synoptic network reports (Fig. 6(d)). Six hours later (at 1200 UTC 4 March) the Balkan front has progressed farther south through the whole of continental Greece and its leading edge is found over central Aegean Sea. Using the hourly outputs of RAMS during the last 24 hours, the progression speed of the Balkan front southwards has been estimated to be 9 m s^{-1}. Strong northerly winds dominate the whole Aegean Sea, with the strongest winds behind the front and intensities well in excess of 20 m s^{-1} (Fig. 9(d)). Negative temperatures are evident over the Balkans and northern Greece, as well as over the mountainous areas of central and southern Greece. Temperatures and winds predicted by RAMS compare favourably with the observations given in Fig. 6(e). Three hours later snow was reported from coastal stations as far south as Athens.

(*b*) *Vertical structure—a density current?*

The vertical structure of the approaching cold outbreak is evident in a north–south oriented vertical cross-section (see Fig. 9(d) for the location of the cross section). Figure 10(a) shows the front-relative northerly wind component at 0000 UTC 4 March 1987 (assuming a frontal speed of approximately 9 m s^{-1} towards the south). The strong northerly flow behind the Balkan front is evident, with a maximum northerly wind of 25 m s^{-1} at approximately 500 m above the ground. Moreover there is a front-relative southerly flow of approximately 25 m s^{-1} in the warm sector, which is evident not only ahead but also above the cold air mass. The leading edge of the front is characterized by a sharp horizontal wind gradient, up to $z = 1000$ m, while the depth of the cold air mass is estimated at 1500 m (if we assume that the top of the cold air was located at the height where the horizontal air motion relative to the front was zero). The same structure is also clear on the temperature cross-section (Fig. 10(b)), with a sharp contrast of 10 °C on the leading edge of the front, and negative values (less than −10 °C) within its cold sector. Six hours later (0600 UTC 4 March), the front has progressed about 180 km to the south (suggesting a propagation speed of about 9 m s^{-1}) with its leading edge still being characterized by strong wind and temperature gradients (Figs. 10(c)–(d)).

Many authors in the past identified the propagation of cold air masses as gravity/density currents (among others: Carbone 1982; Hobbs and Persson 1982; Schoenberger 1984; Chimonas and Kallos 1986; Schultz *et al.* 1997). The speed of a gravity/density current is given by the expression (Carbone 1982; see Bluestein 1993 for the derivation of the formula):

$$c = \left[\frac{K^2 g \Delta z (T_{vw} - T_{vc})}{T_{vc}} \right]^{1/2}, \tag{2}$$

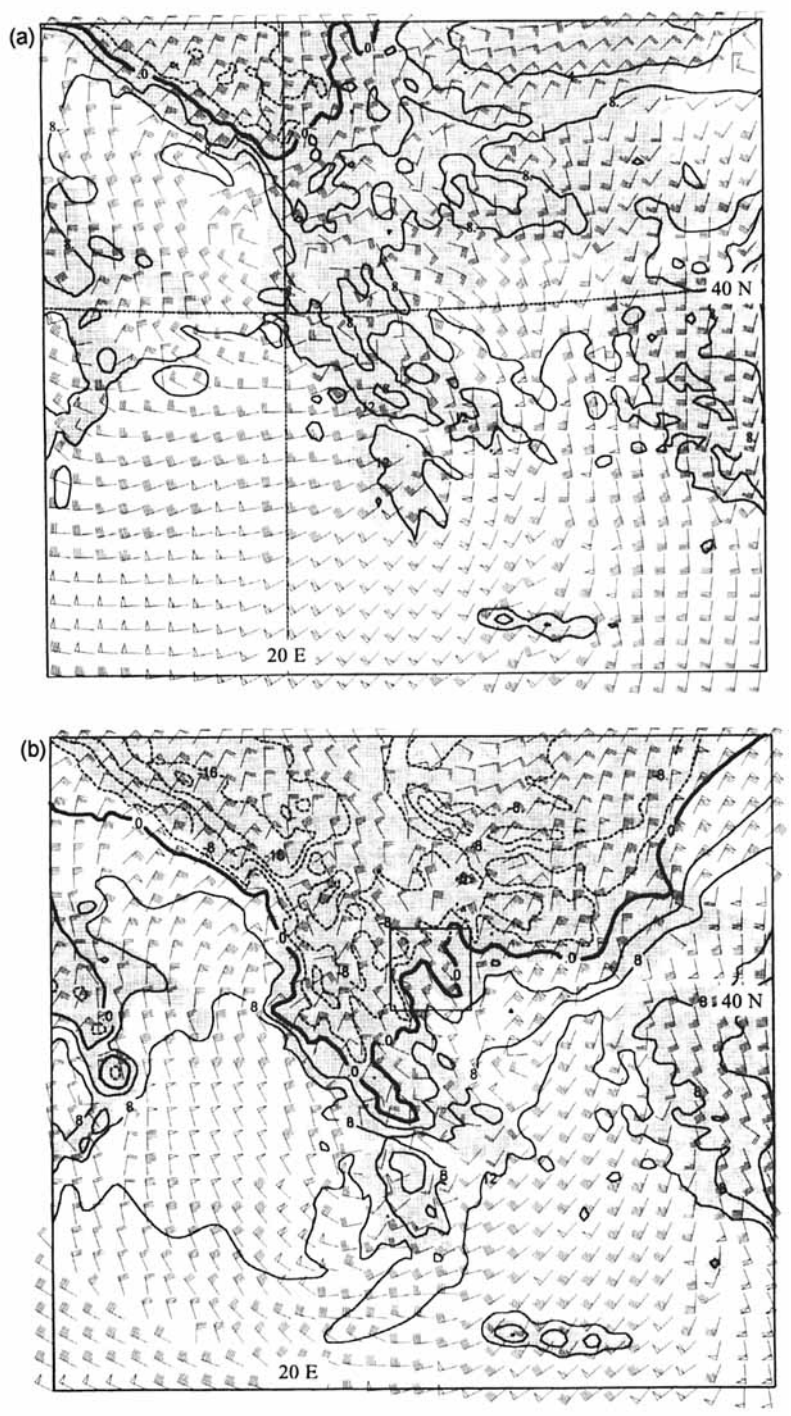

Figure 9. RAMS (see text) predicted temperature (at 4 degC intervals, with negative values dashed) and wind at height $z = 57$ m above ground level (one pennant equals 20 m s^{-1}, one barb 4 m s^{-1} and one half-barb 2 m s^{-1}). Bold lines denote the 0 °C isotherm. Wind symbols are plotted every fourth grid point. (a) 1200 UTC 3 March 1987; (b) 0000 UTC 4 March 1987; the rectangle denotes the area around Vardaris valley (see also Fig. 8); (c) 0600 UTC 4 March 1987; (d) 1200 UTC 4 March 1987; lines AB and CD mark the location of cross-sections shown in Figs. 10 and 12, respectively.

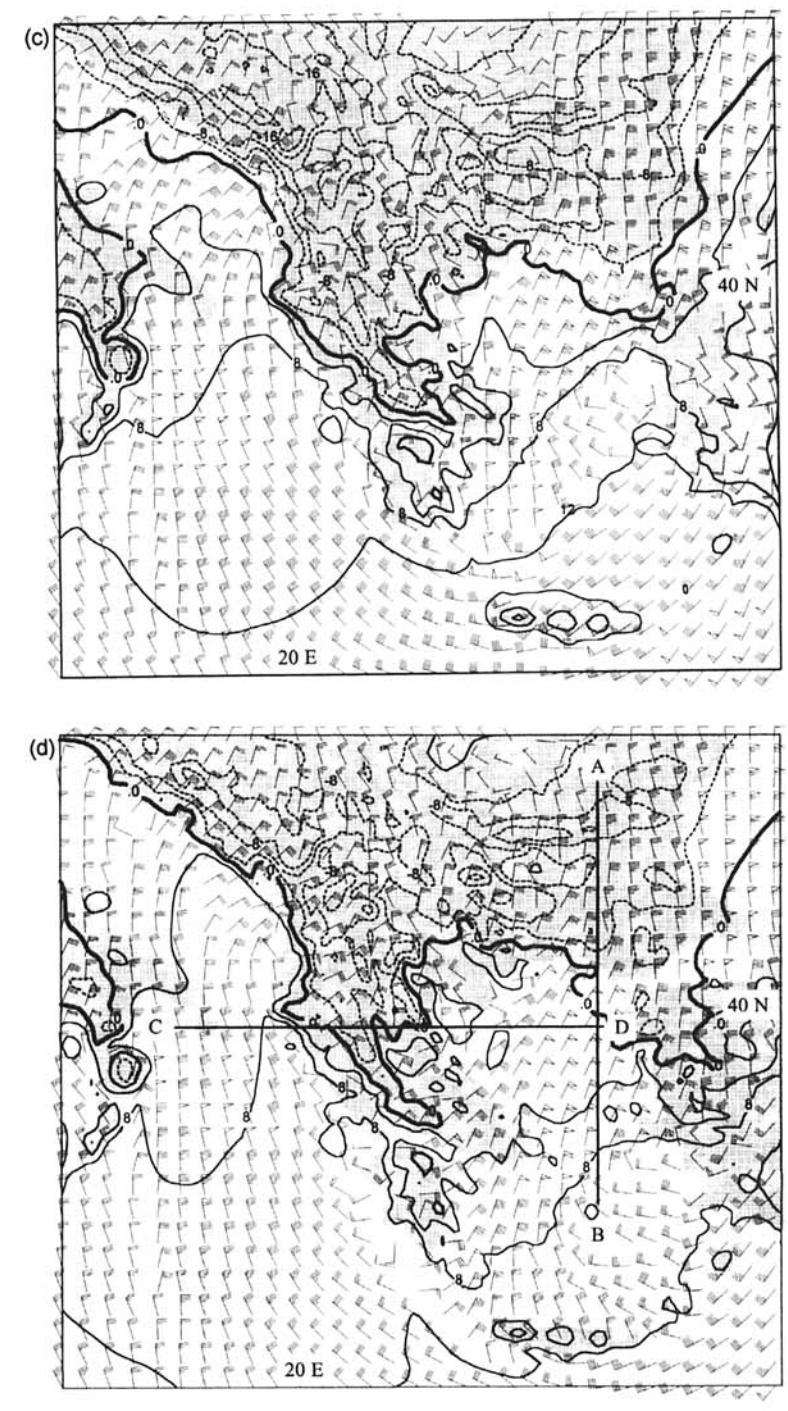

Figure 9. Continued.

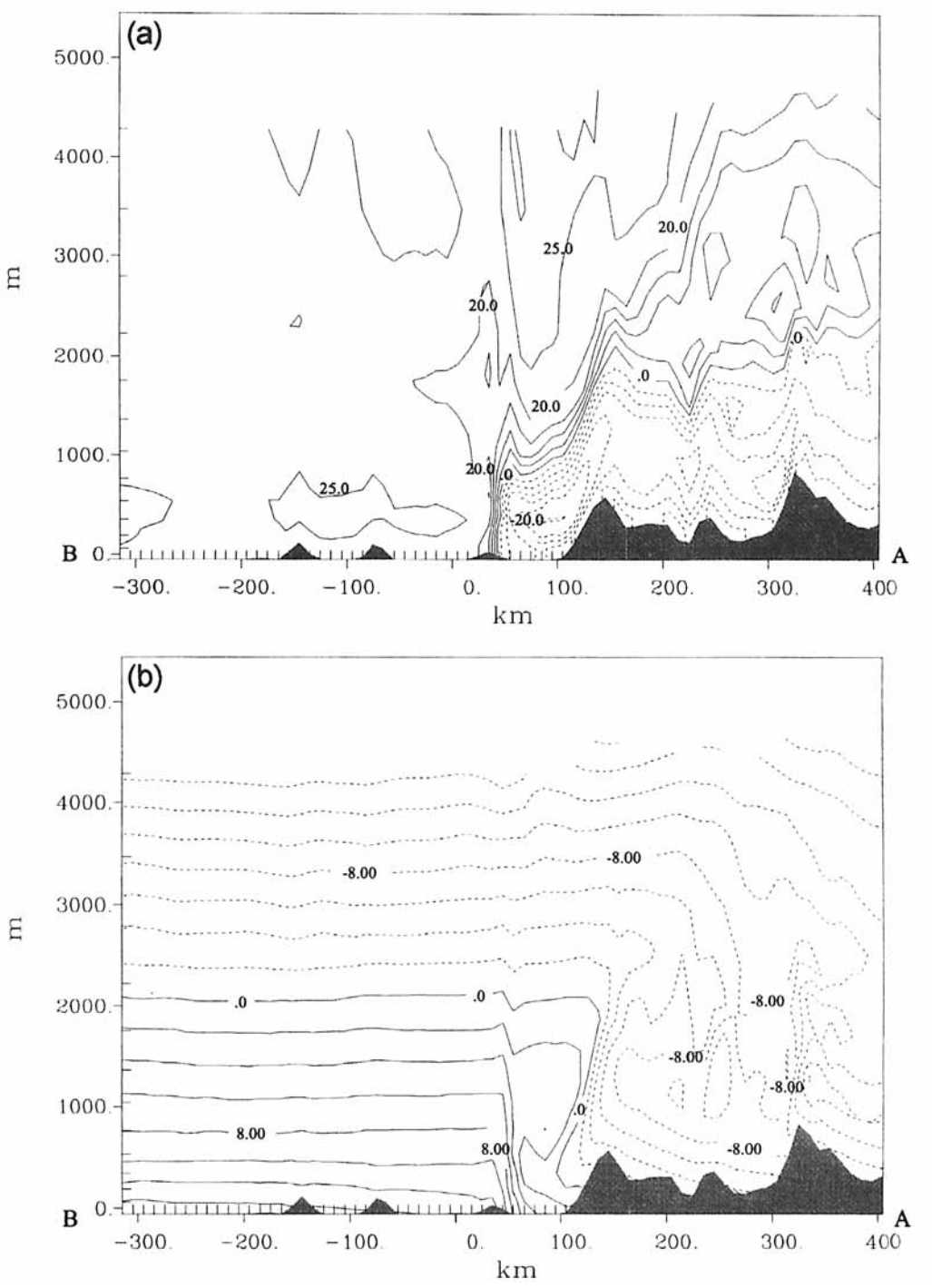

Figure 10. Vertical cross-sections inside the inner grid of RAMS (see text) following the line AB in Fig. 9(d), at 0000 UTC 4 March 1987. (a) The north–south wind component, relative to the moving front (at 5 m s^{-1} intervals, dashed lines denote northerly winds); (b) temperature (at 2 degC intervals); (c) and (d) as (a) and (b), respectively, but at 0600 UTC 4 March 1987.

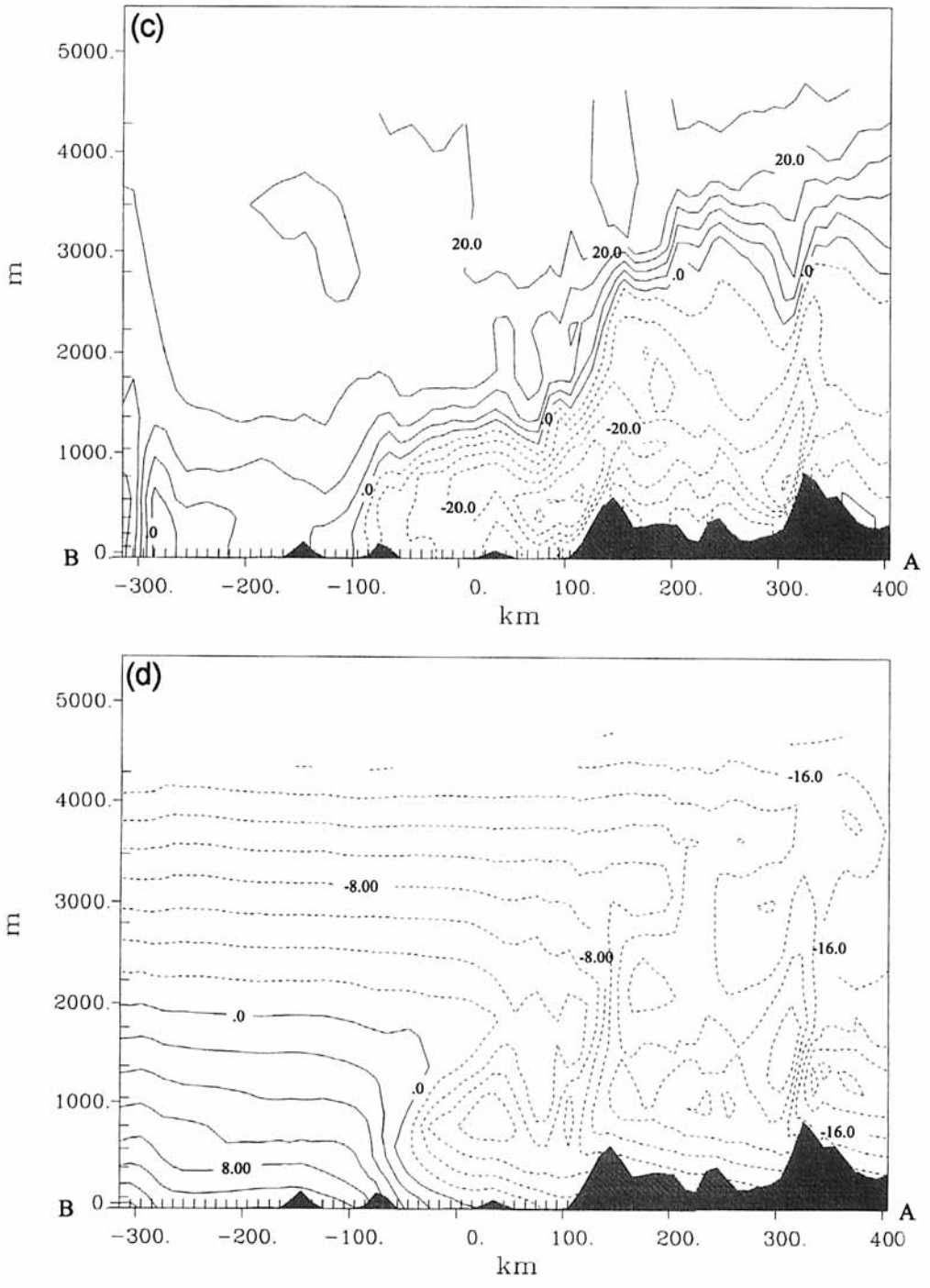

Figure 10. Continued.

where Δz is the depth of the cold-air column, T_{vc} and T_{vw} are the virtual temperature of the cold- and warm-air columns respectively, averaged over Δz, g is the acceleration due to gravity and K is the internal Froude number. Benjamin (1968) and Simpson (1969) have proposed K values between 1 and $\sqrt{2}$, the most appropriate value being 1.1. Estimates of K ranging from 0.6 to 1 have been made in thunderstorm-induced density currents (Bluestein 1993). From Fig. 10(a) the depth of the cold-air column can be estimated as about 1500 m, while inspection of RAMS predicted virtual-temperature fields on the same cross-section (not shown) revealed that $T_{vc} = 268$ K and $T_{vw} = 276$ K. Substitution of these numbers in (2) yields $c = 23$ m s^{-1} for $K = 1.1$. In the warm air there is a front-relative wind component of 25 m s^{-1} in the opposite direction from the Balkan front motion (Fig. 10(a)), which is in good agreement with the value estimated by (2). These calculations suggest that the density-current hypothesis is a likely explanation for the Balkan front motion.

More evidence of the density-current behaviour of the Balkan front is given by the calculation of the pressure rise due to the passage of the cold air over the northern Aegean Sea. Following Schoenberger (1984) and Schultz *et al.* (1997):

$$\Delta P = \frac{P g \Delta z \Delta T_v}{R T_{vw} T_{vc}} \tag{3}$$

where ΔP is the hydrostatic surface-pressure rise behind the front, P is the pre-frontal pressure, $\Delta T_v = T_{vw} - T_{vc}$ and R is the gas constant of dry air. Substituting the values used in the evaluation of (2), and setting $P = 995$ hPa (the report from Limnos island just before the frontal passage), we obtain $\Delta P = 5.5$ hPa, a value which is in very good agreement with the reported pressure rise from Limnos Island of 5.3 hPa between 2100 UTC 3 March and 0000 UTC 4 March (Fig. (5)).

(*c*) *Cold-air damming over the north-western Aegean Sea*

Many researchers have discussed in the past the process of cold-air damming when cold surges move with the topography to the right in the northern hemisphere (Bell and Bosart 1988; Colle and Mass 1995, among others). Cold-air damming refers to the phenomenon of cold air becoming entrenched along the slopes of mountain ranges (Richwien 1980). It is explained by the dynamics of an ageostrophic down-gradient flow forced by an along-barrier pressure gradient, which in its turn has been imposed by the synoptic-scale pressure field (Egger and Hoinka 1992; Overland and Bond 1993; Bluestein 1993; Colle and Mass 1995). The Coriolis force acts to produce a wind component normal to the barrier, leading to the upslope flow of cold air. At low Froude numbers the cold air becomes blocked by the terrain, a cold dome is formed adjacent to the barrier and a strong northerly jet is created (see Fig. 14 in Bell and Bosart 1988). The cold dome is identified by a 'U' shaped ridge in the sea-level pressure pattern and a pronounced temperature trough, while an accelerated flow parallel to the mountains is identified (Bell and Bosart 1988).

Blocking of the flow near mountain ridges is controlled by a Froude number, defined as:

$$F^2 = \frac{U^2}{N^2 H^2} \tag{4}$$

where U is the ambient wind speed, N is the Brunt–Väisälä frequency, and H is the height of the mountain barrier. The square of Froude number expresses an estimate of the ratio of the basic-flow kinetic energy to the energy needed to get an air parcel above the mountain. At small Froude numbers the flow is blocked at low levels, while at large Froude numbers the air flows over the mountains. Blocking of the flow occurs at values ranging from 0.5 to 2.3 (Manins and Sawford 1982). The Froude number values for boundary layer air have

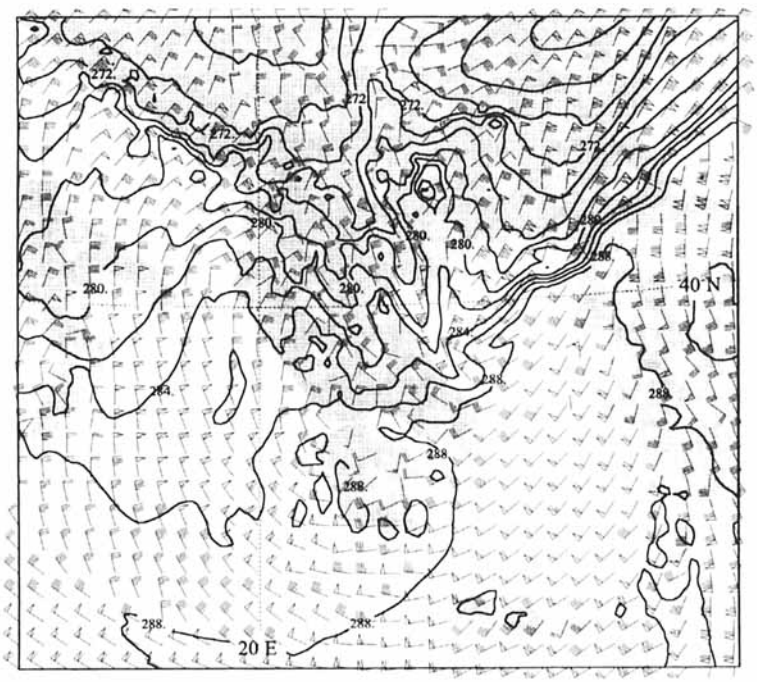

Figure 11. RAMS (see text) predicted potential temperature (at 2 K intervals) and wind at the 925 hPa level, valid at 0000 UTC 4 March 1987. Wind symbols are ploted every fourth grid point; one pennant equals 20 m s^{-1}, one barb 4 m s^{-1} and one half-barb 2 m s^{-1}.

been estimated, based on the model results at 0000 UTC 4 March. Taking the speed of the component of the undisturbed flow normal to the barrier $U = 15$ m s^{-1} (Fig. 12(c)), for a mountain height $H = 1800$ m and a Brunt–Väisälä frequency $N = 0.014$ s^{-1} (estimated from the potential-temperature field given in Fig. 12(a)), yields a Froude number of the order of 0.6. This Froude number implies that the flow was characterized by insufficient energy to flow over the mountain, and thus the system energetics were favourable for cold-air damming.

Figure 11 depicts RAMS potential-temperature and wind fields at 925 hPa. Apart from the aforementioned strong temperature gradient over the north-eastern Aegean Sea, a pronounced temperature trough is evident near the eastern Greek coasts, roughly from 40°N to 39°N. The axis of the temperature trough is approximately parallel to the mountain barrier (Olympus and Ossa mountains to the north, Pelion mountain to the south; see Fig. 8(b) for the location of the mountains). The mountain barrier axis has a north-west to south-east orientation at 35° west of north. The configuration of wind and temperature as well as the shape of sea-level pressure pattern depicted in Fig. 6(c), are very similar to the cold-air damming structure reported by Forbes *et al.* (1987, see their Fig. 7) and Bell and Bosart (1988, see their Fig. 10) east of the Appalachians, as well as Colle and Mass (1995, see their Fig. 16) east of the Rocky Mountains. Moreover a second but less pronounced temperature trough is evident east of Mt. Pindos, corresponding to the pressure ridge over the same location depicted in Fig. 6(c).

The aforementioned authors show cross-sections (normal to the mountain barrier) of the potential temperature and wind which are remarkably similar to RAMS east–west cross-sections at approximately 40°N latitude depicted in Fig. 12. Indeed, at 0000 UTC 4 March 1997 the vertical cross-section of potential temperature reveals the presence of

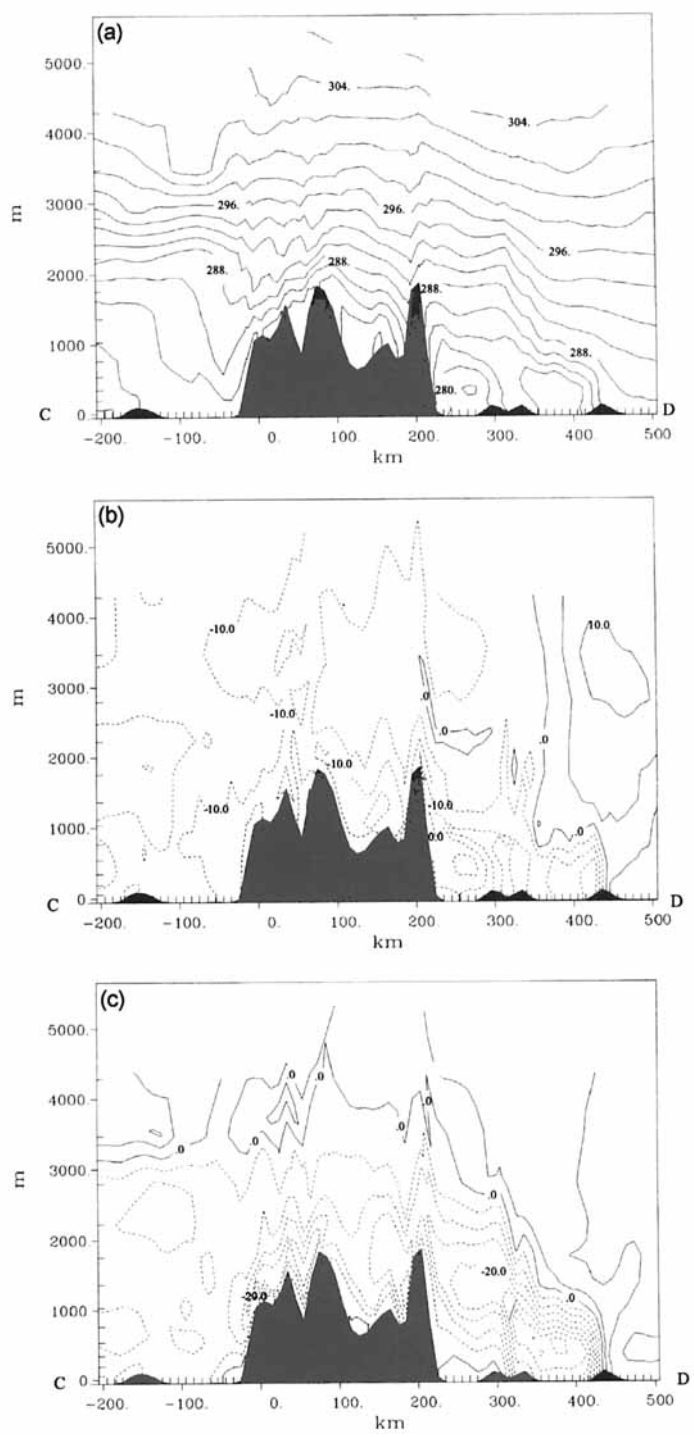

Figure 12. Vertical cross-sections inside the inner grid of RAMS (see text) following the line CD shown in Fig. 9(d), at 0000 UTC 4 March 1987. (a) Potential temperature (at 2 K intervals); (b) wind component parallel to the barrier (at 5 m s^{-1} intervals, dashed lines denote northerly winds); (c) wind component normal to the barrier (at 5 m s^{-1} intervals, dashed lines denote wind towards the mountains).

the cold dome east of Mt. Olympus (Fig. 12(a)), while an important horizontal gradient is evident approximately 200 km offshore. The minimum potential temperature (θ) is 278 K, at $z = 400$ m just east of the barrier. A substantial decrease of potential temperature occurs within the cold dome from a minimum of 284 K at 2000 UTC 3 March to 278 K at 0000 UTC 4 March, and further to 275 K at 0400 UTC 4 March. Inspection of the wind component parallel to the barrier shows the strong component inside the cold dome, exceeding 25 m s^{-1} just east of the barrier and 30 m s^{-1} at 200 km offshore (Fig. 12(b)). Finally, the wind component normal to the barrier (Fig. 12(c)) shows that the flow is oriented towards the barrier, while a reversed flow away from the mountain is evident in a shallow layer near the surface, conforming with theoretical and modelling studies presented in Forbes *et al.* (1987).

All these features indicate that as the Balkan front moved southwards it initiated a pressure gradient along the mountain range, resulting in an ageostrophic flow along the barrier, while the Coriolis force acted to produce an upslope flow (Fig. 12(c)). A low Froude number resulted in the damming of cold air against the mountain and a cold dome was produced (Fig. 12(a)). As a result, a mesoscale pressure ridge formed along the mountains (Figs. 6(c)–(d)). This type of flow interaction with steep topography extends from the barrier over a Rossby radius of deformation (Overland and Bond 1993). Calculation of the Rossby radius of deformation using $(g\Delta\theta H/\theta)^{1/2}/f$ (where $H = 1800$ m, the height of the mountain ridge; $\Delta\theta = 10$ K and $\theta = 280$ K, from the potential-temperature field; Fig. 12(a)) yields a value of 250 km, which is consistent with the horizontal extension of the orographically influenced flow depicted in Fig. 12.

5. Conclusion

This study was devoted to the investigation of the structural evolution and dynamics of the initiation phase of an extreme cold-surge event which affected the Greek peninsula from 3 to 13 March 1987. The persistence of low temperatures and snowfall paralysed the economic and community life of Greece for several days, this event being the worst snowfall over the last 100 years. The analysis was based on inspection of the ECMWF gridded fields and observations from the surface synoptic network, as well as on the results of nested model simulations performed with RAMS.

The cold surge, or Balkan front as it is referred to by Greek forecasters, was associated with a dramatic temperature drop and pressure rise as it moved southwards at an estimated speed to 9 m s^{-1}. The reported 6-hour pressure rise exceeded 10 hPa and the 12-hour pressure rise exceeded 16 hPa on 4 March 1997. The severity of the snowstorm initiation was strongly related to the rapid progression of the Balkan front and the associated pressure rise. This fast changing surface pressure resulted in an important isallobaric wind component, which explains the gustiness of the winds, especially over the northern Aegean Sea. Moreover the resulting highly ageostrophic winds created strong convergence and enhancement of ascending motion, ahead of the rapidly moving front.

The nesting capabilities of RAMS provided information on the scale interaction during this event. The model-forecast dynamic and thermodynamic fields at a fine resolution enabled further insight to be gained into the event, especially over the Greek peninsula. Two important mechanisms associated with the cold surge progression have been identified:

- Over the northern Aegean maritime area the cold-surge progression presented density-current features (with very sharp temperature and horizontal wind gradients evident in the lower tropospheric layers). Indeed, estimation of the hydrostatic pressure rise and speed of the cold surge, based on the density-current theory, was in good agreement with the observations.

• On the other hand, the progression of the Balkan front over the eastern coast of continental Greece was orographically influenced. Indeed, the along-barrier pressure gradient lead to an accelerated flow parallel to the mountains advecting cold air along the eastern slopes of the mountain barrier. The Coriolis force acted on this ageostrophic down-gradient flow and produced an upslope component of the flow at the leading edge of the surge. The flow was characterized by a low Froude number value ($F = 0.6$) and, as the cold air had unsufficient energy to flow over the barrier, it was trapped ('dammed') on the eastern side of the mountain and a cold dome was formed (in very good agreement with observations of such events provided in the literature). Moreover the pressure-field adjustment in low tropospheric layers resulted in the development of a mesoscale ridge along the eastern slopes of the Greek peninsula mountains.

Additional model and observational studies of the progression of cold surges over the Greek peninsula would be necessary in order to be sure of the role of cold-air damming over the mountain barriers along eastern Greece, and to derive conceptual models of the Balkan front progression.

Acknowledgements

The authors are grateful to Mr D. Ziakopoulos (Hellenic Meteorological Service) and to Dr Y. Lemaitre (CETP-IPSL, France) for their helpful suggestions. Mrs M. Varinou (University of Athens) is also acknowledged for helpful discussions. Acknowledgement is also made to Dr T. Hewson (Meteorological Office, UK) for providing the frontal objective analysis code, and to the National Center for Atmospheric Research, which is sponsored by the National Science Foundation (USA), for some of the computing time used in this research and for providing the sounding and surface data from the operational network (Contract #35081178), also to the Hellenic Meteorological Service for providing surface observations. This study was partially supported by SKIRON (EPET II - 322) program of the Greek Secretariat of Research and Technology.

References

Avissar, R. and Mahrer, Y. 1988 Mapping frost sensitive areas with a three dimensional local scale numerical model. Part I: Physical and numerical aspects. *J. Appl. Meteorol.*, **27**, 400–413

Bell, G. D. and Bosart, L. F. 1988 Appalachian cold-air damming. *Mon. Weather Rev.*, **116**, 137–161

Benjamin, T. B. 1968 Gravity currents and related phenomena. *J. Fluid Mech.*, **31**, 209–248

Bluestein, H. B. 1993 Synoptic–dynamic meteorology in midlatitudes. P. 431 in *Volume I: Principles of kinematics and dynamics*. Oxford University Press

Browning, K. A. and Pardoe, C. W. 1973 Structure of low-level jet streams ahead of midlatitude cold fronts. *Q. J. R. Meteorol. Soc.*, **99**, 619–638

Carborne, R. E. 1982 A severe frontal rainband. Part I: Stormwide hydrodynamic structure. *J. Atmos. Sci.*, **39**, 258–279

Chen, C. and Cotton, W. R. 1987 The physics of the marine stratocumulus-capped mixed layer. *Boundary-Layer Meteorol.*, **25**, 289–321

Chimonas, G. and Kallos, G. 1986 Flow dynamics and stability in a severe rainband. *J. Atmos. Sci.*, **43**, 1505–1516

Clark, T. L. and Farley, R. D. 1984 Severe downslope windstorm calculations in two and three spatial dimensions using anelastic interactive grid nesting: A possible mechanism for gustiness. *J. Atmos. Sci.*, **41**, 329–350

Colle, B. A. and Mass, C. F. 1995 The structure and evolution of cold surges east of the Rocky mountains. *Mon. Weather Rev.*, **123**, 2577–2610

Cotton, W. B., Thompson, T. and Mielke, P. W. 1994 Real time mesoscale prediction on workstations. *Bull. Am. Meteorol. Soc.*, **75**, 349–362

Davies, H. C.	1976	A lateral boundary formulation for multi-level prediction models. *Q. J. R. Meteorol. Soc.*, **102,** 405–418
Egger, J. and Hoinka, K. P.	1992	Fronts and orography. *Meteorol. Atmos. Phys.*, **48,** 3–36
Forbes, G. S., Anthes, R. A. and Thomson, D. W.	1987	Synoptic and mesoscale aspects of an Appalachian ice storm associated with cold-air damming. *Mon. Weather Rev.*, **115,** 564–591
Hewson, T. D.	1996	'Objective Fronts'. Internal Report 57, Joint Centre for Mesoscale Meteorology, Reading University, UK
Hobbs, P. V. and Persson, P. O. G.	1982	The mesoscale and microscale structure and organization of clouds and precipitation in midlatitude cyclones. Part V: The substructure of narrow cold frontal rainbands. *J. Atmos. Sci.*, **39,** 280–295
Kallos, G. and Metaxas, D.	1980	Synoptic processes for the formation of Cyprus lows. *Riv. Meteorol. Aer.*, XL, 2, 121–138
Livada-Tselepidaki, H.	1979	'Snowfalls in Greece'. PhD. thesis, University of Athens (in Greek)
McCumber, M. C. and Pielke, R. A.	1981	Simulation of the effects of surface fluxes of heat and moisture in a mesoscale numerical model. Part I: Soil layer. *J. Geophys. Res.*, **86,** 9929–9938
Manins, P. C. and Sawford, B. L.	1982	Mesoscale observations of upstream blocking. *Q. J. R. Meteorol. Soc.*, **108,** 427–434
Metaxas, D.	1978	Strong cold outbreaks in the East Mediterranean. A synoptic study. *Riv. Meteorol. Aer.*, XXXVIII, **3,** 95–105
Meteorological Office	1962	Weather in the Mediterranean, *Vol. I, General Meteorology*. H.M.S.O., London. Second Edition
Nakamura, H. and Murakami, T.	1983	Orographic effects on cold surges and lee-side cyclogenesis as revealed by a numerical experiment, Part II, transient aspects. *J. Meteorol. Soc. Jpn*, **61,** 547–567
Overland, J. E. and Bond, N.	1993	The influence of coastal orography: The Yakutat storm. *Mon. Weather Rev.*, **121,** 1388–1397
Pielke, R. A., Cotton, W. R., Walko, R. L., Tremback, C. J., Lyons, W. A., Grasso, L. D., Nicholls, M. E., Moran, M. D., Wesley, D. A., Lee, T. J. and Copeland, J. H.	1992	A comprehensive meteorological modelling system—RAMS. *Meteorol. Atmos. Phys.*, **49,** 69–91
Prezerakos, N. and Angouridakis, V.	1984	Synoptic consideration of snowfall in Athens. *J. Climatol.*, **4,** 269–285
Richwien, B. A.	1980	The damming effect of the southern Appalachians. *Natl. Weather Dig.*, **5**(1), 2–12
Schoenberger, L. M.	1984	Doppler radar observation of a land-breeze cold front. *Mon. Weather Rev.*, **112,** 2455–2464
Schultz, D. M., Bracken, W. E., Bosart, L. F., Hakim, G. J., Bedrick, M. A., Dickinson, M. J. and Tyle, K. R.	1997	The 1993 superstorm cold surge: frontal structure, gap flow and tropical impact. *Mon. Weather Rev.*, **125,** 5–39
Simpson, J. E.	1969	A comparison between laboratory and atmospheric density currents. *Q. J. R. Meteorol. Soc.*, **95,** 758–765
Tremback, C. J.	1990	Numerical simulation of a mesoscale convective complex: Model development and numerical results. Ph.D. dissertation, Atmos. Sci. Paper No. 465, Colorado State University, Dept. of Atmos. Science, Fort Collins, Co 8523
Tremback, C. J., Lyons, W. A., Cotton, W. R., Walko, R. L. and Beitler, B.	1994	'Operational weather forecasting applications using the Regional Atmospheric Modelling System (RAMS)'. Preprints of the 10th Conference on Numerical Weather Prediction, 18–22 July 1994, Portland, OR
Walko, R. L., Cotton, W. R., Meyers, M. P. and Harrington, J. Y.	1995	New RAMS cloud microphysics parameterization. Part I: the single moment scheme. *Atmos. Res.*, **38,** 29–62